Title: Early Universe phenomenology after BICEP

Date: Apr 04, 2014 03:20 PM

URL: http://pirsa.org/14040125

Abstract:

Early Universe phenomenology after BICEP

April 2014
Perimeter Institute

$$\frac{1}{2}m^2\phi^2$$

$$V^{1/4} \approx 10^{16}\mathrm{GeV}$$

$$\dot{\phi}^{1/2} \approx 10^{15}\mathrm{GeV}$$

$$H \approx 10^{14}\mathrm{GeV}$$

$$m \approx 10^{13}\mathrm{GeV}$$

$$\Delta\phi \simeq 15\, M_{\mathrm{pl}}$$

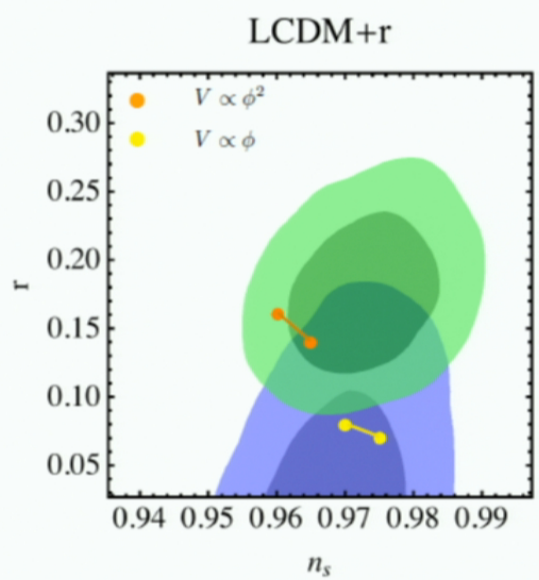

(Spectra, covariance matrix from Spergel, Flauger, Hlozek 2013)

"The tension"

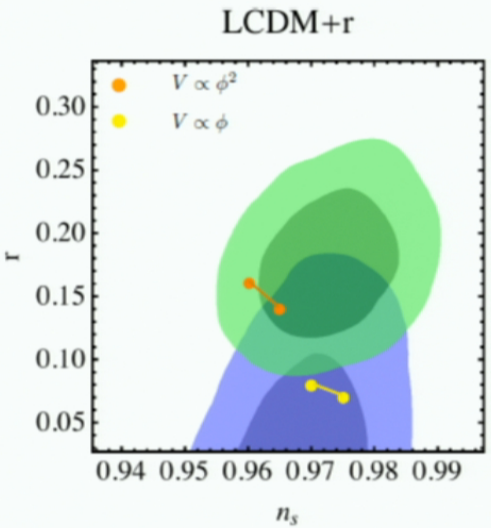

(Spectra, covariance matrix from Spergel, Flauger, Hlozek 2013)

- Running (seems like the best time to give up slow roll-inflation)
- A brake in the spectrum (Evidence for the multiverse (perhaps the MUH?))
- nt > 0 (good news for string gas cosmology)

Are the B modes primordial? Defects

Moss & Pogosian1403.6105

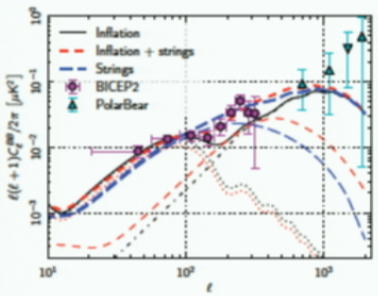

FIG. 1. The thick blue long dashed line is the best fit lensing+strings model (r=0), with the thin blue long dashed line showing the corresponding string contribution alone. The thick red short dash is the best fit lensing+strings+inflation model (r=0.15), with the corresponding string contribution plotted as a thin red short dashed line. The lensing contribution is shown separately with a thin black dot-dashed line. The BICEP2 best fit inflationary model (r=0.2) contribution is shown with a thin black dotted line, and the solid thin black line is the sum of r=0.2 and lensing contributions. The circles show the band powers measured by BICEP2 and the triangles are the POLARBEAR data (the third band is negative with its absolute value plotted as an inverted triangle).

Lizarraga et al 1403.4924

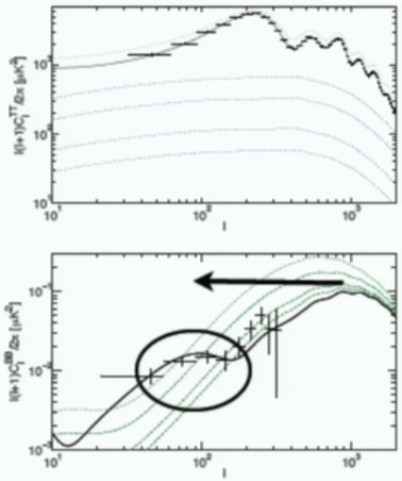

FIG. 3: Temperature (upper panel) and B-mode polarization (lower panel) power spectra compared to the *Planck* temperature and the BICEP2 B-mode polarization data. The black curve in the upper panel is the best-fit ΛCDM model and the blue dashed lines show the contribution from strings for $f_{10} = 0.3$, 0.15, 0.06, and 0.03. The green-dotted curves in the lower panel show the combined contribution from strings and the lensing of the scalar perturbations, for the same values of f_{10} as in the upper panel. The lowest dotted curve, for $f_{10} = 0.03$, shows roughly the maximal allowed contribution from strings to the temperature power spectrum, given the *Planck* data. The highest dotted curve, $f_{10} = 0.3$, matches the BICEP2 B-mode polarization at $\ell = 80$. The grey dashed line is the sum of the $f_{10} = 0.3$ string prediction with the *Planck* best-fit ΛCDM model.

$$\Delta\theta \approx 2^o$$

Location of peak constrained by Causality.

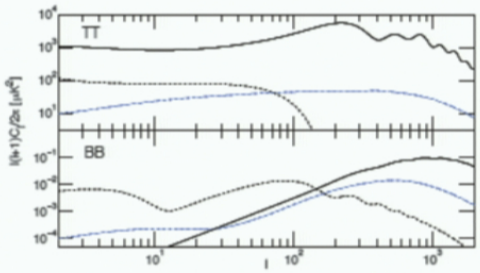

FIG. 1: The CMB temperature and polarization power spectra contributions from inflationary scalar modes (black solid), inflationary tensor modes (black dashed), and cosmic strings (blue dot-dashed) [16]. The inflationary tensors have r = 0.2 while the string contribution has $f_{10} = 0.03$.

$$C_{Bl} = 2\pi \int_0^{\pi} \theta d\theta \, \{[C_Q(\theta) + C_U(\theta)] \, J_0(l\theta) - [C_Q(\theta) - C_U(\theta)] \, J_4(l\theta)\}$$

Direct test

Baumann & MZ 0901.0958

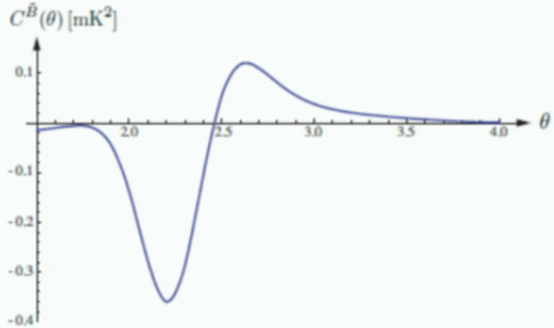

Figure 3: $C^{\hat{B}}(\theta) = \langle \hat{B}\hat{B} \rangle(\theta)$: real space correlation function on superhorizon scales. $C^{\hat{B}}(\theta \gtrsim 2^\circ) \neq 0$ is a unique signature of inflationary tensor modes.

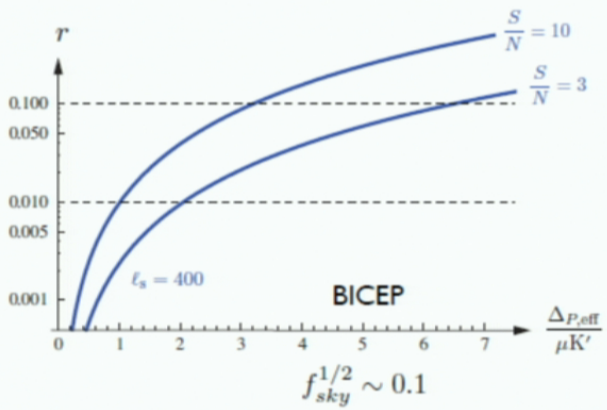

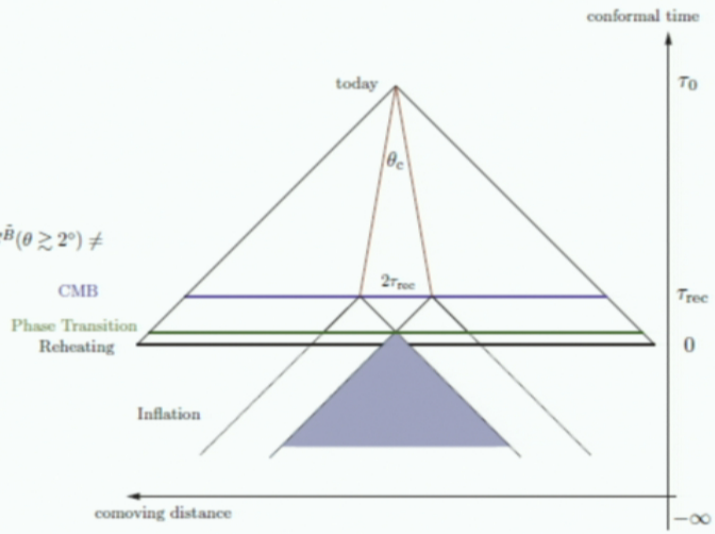

Figure 1: Causal structure of the universe. Correlations between any local variables at any two spacetime points vanish if their backward light cones fail to intersect on the spacelike hypersurface Σ corresponding to the phase transition at $\tau = \tau_{\mathrm{pt}}$ [14]. On the surface of last-scattering at τ_{rec} this corresponds to angular separations $\theta > \theta_c \approx 2^\circ$. Longer range correlations are established during inflation at negative values of conformal time, $\tau < 0$.

Other sources of GW during inflation

Senatore, Silverstein and MZ

$$\dot{\phi}^2 >> H^4$$

Perhaps you can tap to this source of energy and create some GW.

Example: inflaton creates massive particles which emit GW when they decay.

$$h^2 \sim \frac{fHM}{M_{pl}^2}$$

Be careful: You also create scalars

$$r = 16\epsilon \rightarrow 16\epsilon\alpha \sim 16\epsilon^2$$

BICEP level so large that it is difficult to hide the scalars. They must be the ones we observe $\rightarrow \epsilon \sim 0.1$

Need to worry about Gaussianity $N_\phi^{1/2} \sim N_h^{1/2} \sim (\frac{h^2}{H^2/M_{pl}^2})^{1/2} > 10^3$

Saturating all the values of the parameters we were getting more than this by one or two orders of magnitude.

Other sources of GW during inflation

Senatore, Silverstein and MZ

$\dot{\phi}^2 >> H^4$

Perhaps you can tap to this source of energy and create some GW.

Example: inflaton creates massive particles which emit GW when they decay.

$h^2 \sim \frac{fHM}{M_{pl}^2}$

Be careful: You also create scalars

$r = 16\epsilon \rightarrow 16\epsilon\alpha \sim 16\epsilon^2$

BICEP level so large that it is difficult to hide the scalars. They must be the ones we observe $\rightarrow \epsilon \sim 0.1$

Need to worry about Gaussianity $N_\phi^{1/2} \sim N_h^{1/2} \sim (\frac{h^2}{H^2/M_{pl}^2})^{1/2} > 10^3$

Saturating all the values of the parameters we were getting more than this by one or two orders of magnitude.

Enhanced scalar fluctuations

Speed of sound

$$r = 16\epsilon c_s$$

$$n_s - 1 \subset 6\epsilon$$

BICEP $\longrightarrow$ $q \sim 1$, $c_s \sim 1$

Second field (curvaton/variable reheating)

$$r = 16\epsilon q$$

$$q = \frac{P_\zeta^\phi}{P_\zeta^\phi + P_\zeta^\sigma}$$

$$n_s - 1 \subset 2\epsilon$$

(non-G Planck)

$c_s > 0.02$ $\longrightarrow$ $\epsilon \sim 1$

non-G no longer useful to constrain cs

Implications for non-Gaussianity

Local non-Gaussianity from conversion

$$\zeta(x) = \left.\frac{\partial\zeta}{\partial\pi}\right|_0 \pi(x) + \left.\frac{\partial\zeta}{\partial\sigma_I}\right|_0 \sigma_I(x) + \frac{1}{2!}\left.\frac{\partial^2\zeta}{\partial\pi^2}\right|_0 \pi(x)^2 + \frac{1}{2!}\left.\frac{\partial^2\zeta}{\partial\pi\partial\sigma_I}\right|_0 \pi(x)\sigma_I(x) + \frac{1}{2!}\left.\frac{\partial^2\zeta}{\partial\sigma_I\partial\sigma_J}\right|_0 \sigma_I(x)\sigma_J(x) + \frac{1}{3!}\left.\frac{\partial^3\zeta}{\partial\sigma_I\partial\sigma_J\partial\sigma_K}\right|_0 \sigma_I(x)\sigma_J(x)\sigma_K(x) + \dots .$$

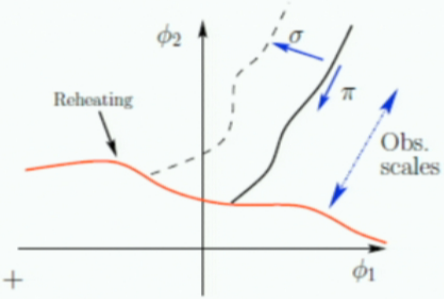

$$\zeta = \zeta_\phi + \zeta_\sigma + f_{\rm nl}\zeta_\sigma^2$$

$$NG^\sigma = f_{\rm nl}\zeta_\sigma < 1$$

$$\frac{\langle\zeta^3\rangle}{\langle\zeta^2\rangle^{3/2}} = NG^\zeta = NG^\sigma(1-q)^{3/2} \approx NG^\sigma\left(\frac{P_\zeta^\sigma}{P_\zeta^\phi}\right)^{3/2}$$

Even a component that contributes very little to the two point function could lead to a measurable non-Gaussianity.

If it contributes 1% to the power it saturates current non-G constraints if it is very non-Gaussian.

Non-G in the EFT

$$S = \int d^4x \sqrt{-g} \; \Big[\; \frac{1}{2} M_{\rm Pl}^2 R + M_{\rm Pl}^2 \dot{H} g^{00} - M_{\rm Pl}^2 (3H^2 + \dot{H}) + \\ + \frac{1}{2!} M_2(t)^4 (g^{00}+1)^2 + \frac{1}{3!} M_3(t)^4 (g^{00}+1)^3 + \\ - \frac{\bar{M}_1(t)^3}{2} (g^{00}+1) \delta K^\mu{}_\mu - \frac{\bar{M}_2(t)^2}{2} \delta K^\mu{}_\mu{}^2 - \frac{\bar{M}_3(t)^2}{2} \delta K^\mu{}_\nu \delta K^\nu{}_\mu + \ldots \Big]$$

$$g^{00} \quad \to \quad -1 - 2\dot{\pi} - \dot{\pi}^2 + \frac{1}{a^2} (\partial_i \pi)^2$$

$$S_\pi = \int d^4x \sqrt{-g} \left[-M_{\rm Pl}^2 \dot{H} \left(\dot{\pi}^2 - \frac{(\partial_i \pi)^2}{a^2} \right) + 2 M_2^4 \left(\dot{\pi}^2 + \dot{\pi}^3 - \dot{\pi} \frac{(\partial_i \pi)^2}{a^2} \right) - \frac{4}{3} M_3^4 \dot{\pi}^3 + \ldots \right]$$

c_s^2 $\qquad$ $f_{\rm NL} \sim \frac{1}{c_s^2}$

Small cs implies large non-G.

$$M_2^4 \to M_3^4$$

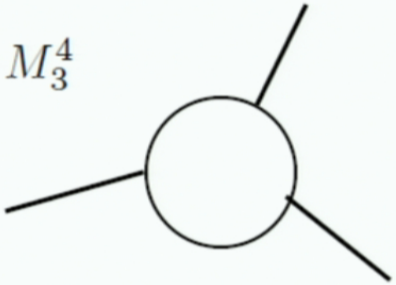

$$\frac{1}{\Lambda_2^2} \dot{\pi}_c \frac{(\tilde{\partial}_i \pi)^2}{a^2} \to \frac{1}{\Lambda_2^2} \dot{\pi}_c^3$$

If I run the loop to the cut-off will generate an M3 term that leads to the same strength of non-G.

Non-G in the EFT

Can I have large non-G without touching cs?

$$M_3^4 \to M_2^4 \qquad (\dot\pi + \frac{1}{2}\dot\pi^2 - \frac{1}{2}\partial_i\pi^2)^3 \to \dot\pi^3 - \frac{3}{2}\dot\pi^2\partial_i\pi^2 + \cdots$$

$$\frac{1}{\Lambda_2^2}\dot\pi_c^3 \to \frac{1}{(|\dot H|M_{pl}^2)^{1/2}}\dot\pi_c\frac{(\tilde\partial_i\pi)^2}{a^2}$$

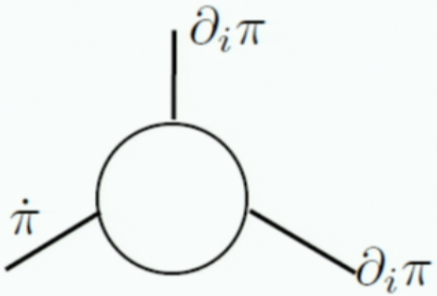

$$\Delta c_s \sim 1$$

Large non-G does not imply small cs, even if I run the loop all the way to the cut-off the expected correction to cs is of order one.

This is fine with current data but probably not in the future.

Other Light fields

- Local type non-Gaussianities
- wide range of behavior in the squeezed limit.
- Different shapes than those that can be produced by single field
- 4-pt functions with large signal to noise

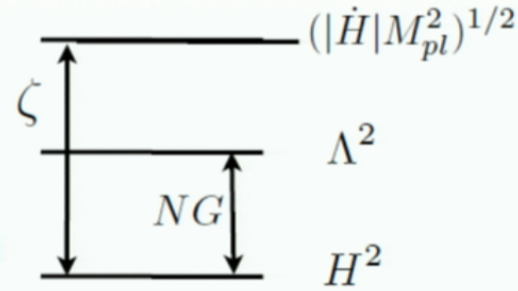

EFT of multifield inflation 1009.2093

Operator	Dispersion		Type	Origin	Squeezed L.
	$w = c_s k$	$w \propto k^2$			
$\dot\sigma^4$, $\dot\sigma^2(\partial_i\sigma)^2$,$(\partial_i\sigma)^4$	X		Ad., Iso.	Ab., non-Ab.	
$(\partial_\mu\sigma)^4$	X		Ad., Iso.	Ab., non-Ab.	
$\dot\sigma^p(\partial_i\partial_j\sigma)^{(4-p)}$		X	Ad., Iso.	Ab.	
σ^4	X	X	Ad., Iso.	Ab.$_*$, non-Ab.$_*$, S.	X
$\dot\sigma\sigma^3$	X	X	Ad., Iso.	Ab.$^\dagger_*$, non-Ab.$^\dagger_*$.	X
$\sigma^2\dot\sigma^2$,$\sigma^2(\partial_i\sigma)^2$	X	X$^{\dagger *}$	Ad.$^{\dagger *}$, Iso.	non-Ab, Ab.$^{\dagger *}_*$, non-Ab.$^{\dagger *}_*$.	X
$\sigma^2(\partial_\mu\sigma)^2$	X		Ad.$^{\dagger *}$, Iso.	non-Ab, Ab.$^{\dagger *}_*$, non-Ab.$^{\dagger *}_*$, S.*	X
$\sigma(\partial\sigma)^3$	X		Iso.	non-Ab.$^*_*$.	X
$\dot\sigma^3$, $\dot\sigma(\partial_i\sigma)^2$	X		Ad., Iso.	Ab., non-Ab.	
$\dot\sigma(\partial_i\sigma)^2$,$\partial_i^2\sigma(\partial_i\sigma)^2$		X	Ad., Iso.	Ab.	
σ^3	X	X	Ad., Iso.	Ab.$_*$, non-Ab.$_*$, S, R	X
$\dot\sigma\sigma^2$	X	X	Ad., Iso.	Ab.$_*$, non-Ab.$_*$	X
$\sigma\dot\sigma^2$, $\sigma(\partial_i\sigma)^2$	X	X	Ad., Iso.	Ab.$^\dagger_*$, non-Ab.$^\dagger_*$	X
$\sigma(\partial_\mu\sigma)^2$	X		Ad., Iso.	Ab.$^\dagger_*$, non-Ab.$^\dagger_*$.	X

Table 1: Signatures in Multi-field Inflation. In the first column we give the operator generating the non-Gaussian signal: operators quartic in the σ's lead to a four-point function, operators cubic in the σ's lead to a three-point function. In the second and third columns we explain with which dispersion relation the signal can be generated. In the third we explain if the signal can appear in the Adiabatic (Ad.) or the Isocurvature (Iso.) fluctuations. In the fourth we state the potential origin of the signal. Here Ab. stands for Abelian; non-Ab. stands for non-Abelian, S stands for supersymmetry, and R stands for generated by non-linearities at reheating. The subscript $_*$ indicates that the term is generated by soft-breaking terms. The symbol † represents that such a signal can be generated in the case the soft symmetry breaking term is such that it forbids some of the lowest dimensional terms. The symbol * represents the fact that the signal is in general subleading, but still possibly detectable. In the last column we explicitly mention if the induced signal has a non-vanishing squeezed limit and is therefore detectable also in clustering statistics of collapsed objects.

Signatures of SUSY from the Early Universe1109.0292

Table 1: *Non-Gaussianity in Quasi-Single Field Inflation.*

Interaction	$f_{\rm NL}^{(1)}$	$f_{\rm NL}^{(2)}$	Large NG	S.L.	SUSY	Natural
$\mathcal{L}_{1a} = m_a^3(\partial_\mu\pi)^2\sigma$	$\left(\frac{\rho}{H}\right)^2$	$\alpha\,\frac{\rho}{H}$		✓	✓	
$\mathcal{L}_{1b} = m_b^3(\dot\pi)^2\sigma$	$\left(\frac{\rho}{H}\right)^2$	$\alpha\,\frac{\rho}{H}$		✓	✓	
$\mathcal{L}_2 = \dot m^2(\partial_\mu\pi)^2\dot\sigma$	$\frac{\rho}{H}\,\alpha$	α^2				
$\mathcal{L}_3 = \ddot m^2\dot\pi\sigma^2$	$\left(\frac{\rho}{H}\right)^2\left(\frac{m}{H}\right)^2$	$\alpha^2\left(\frac{m}{H}\right)^2$		✓		
$\mathcal{L}_{4a} = \dot m_a\partial_\mu\pi\partial^\mu\sigma\sigma$	$\left(\frac{\rho}{H}\right)^2\frac{m_a}{H}$	$\alpha^2\frac{m_a}{H}$		✓	✓	
$\mathcal{L}_{4b} = \dot m_b\dot\pi\dot\sigma\sigma$	$\left(\frac{\rho}{H}\right)^2\frac{m_b}{H}$	$\alpha^2\frac{m_b}{H}$		✓		
$\mathcal{L}_{5a} = \lambda_a\dot\pi(\partial_\mu\sigma)^2$	$\left(\frac{\rho}{H}\right)^2\lambda_a$	$\alpha^2\lambda_a$				
$\mathcal{L}_{5b} = \lambda_b\partial_\mu\pi\partial^\mu\sigma\dot\sigma$	$\left(\frac{\rho}{H}\right)^2\lambda_b$	$\alpha^2\lambda_b$				
$\mathcal{L}_{5c} = \lambda_c\dot\pi\dot\sigma^2$	$\left(\frac{\rho}{H}\right)^2\lambda_c$	$\alpha^2\lambda_c$				
$\mathcal{L}_6 = \mu\sigma^3$	$\left(\frac{\rho}{H}\right)^3\frac{\mu}{H}\Delta_\zeta^{-1}$	$\alpha^3\frac{\mu}{H}\Delta_\zeta^{-1}$	✓	✓	✓	✓
$\mathcal{L}_7 = \lambda\dot\sigma\sigma^2$	$\left(\frac{\rho}{H}\right)^3\lambda\,\Delta_\zeta^{-1}$	$\alpha^3\lambda\,\Delta_\zeta^{-1}$	✓	✓		(?)
$\mathcal{L}_{8a} = \Lambda_1^{-1}(\partial_\mu\sigma)^2\sigma$	$\left(\frac{\rho}{H}\right)^3\frac{H}{\Lambda_1}\Delta_\zeta^{-1}$	$\alpha^3\frac{H}{\Lambda_1}\Delta_\zeta^{-1}$	✓	✓	✓	✓
$\mathcal{L}_{8b} = \Lambda_2^{-1}\dot\sigma^2\sigma$	$\left(\frac{\rho}{H}\right)^3\frac{H}{\Lambda_2}\Delta_\zeta^{-1}$	$\alpha^3\frac{H}{\Lambda_2}\Delta_\zeta^{-1}$	✓	✓		(?)
$\mathcal{L}_{9a} = \Lambda_3^{-2}\dot\sigma(\partial_\mu\sigma)^2$	$\left(\frac{\rho}{H}\right)^3\left(\frac{H}{\Lambda_3}\right)^2\Delta_\zeta^{-1}$	$\alpha^3\left(\frac{H}{\Lambda_3}\right)^2\Delta_\zeta^{-1}$	✓			✓
$\mathcal{L}_{9b} = \Lambda_4^{-2}\sigma^3$	$\left(\frac{\rho}{H}\right)^3\left(\frac{H}{\Lambda_4}\right)^2\Delta_\zeta^{-1}$	$\alpha^3\left(\frac{H}{\Lambda_4}\right)^2\Delta_\zeta^{-1}$	✓			✓

QSF dynamics with large non-G

(Xingang Chen)

$$\frac{\dot{\phi}}{\Lambda H}$$

Mixing

$$\mathcal{L}_\sigma = -\tfrac{1}{2}[\partial_\mu\sigma\partial^\mu\sigma + m^2\sigma^2] - \mu\sigma^3 + \frac{\sigma}{\Lambda}[\partial_\mu\phi\partial^\mu\phi - \langle\dot{\phi}\rangle^2]$$

$$\left(\frac{\dot{\phi}}{\Lambda H}\right) \sim \epsilon^{1/2}\left(\frac{M_{pl}}{\Lambda}\right)$$

$$\frac{f_{\rm NL}^{\rm equil.}}{75} \sim 12\,\frac{\mu}{H}\left(\frac{r}{0.2}\right)^{1/2}\left(\frac{M_{\rm pl}}{\Lambda}\right)^3$$

$$f_{\rm NL}^{\rm equil.} = -42 \pm 75 \ \ (\text{at } 1\sigma)$$

Current constraint from Planck

Testing Split Supersymmetry with Inflation

Nathaniel Craig♠ and Daniel Green♦♣

Planck-Suppressed Operators

Valentin Assassi,★ Daniel Baumann,★ Daniel Green,♦♣ and Liam McAllister♠

The future?

Deviation from the line

$$(n_s - 1) + \frac{r}{4} + \frac{11}{24}(n_s - 1)^2 = 0$$

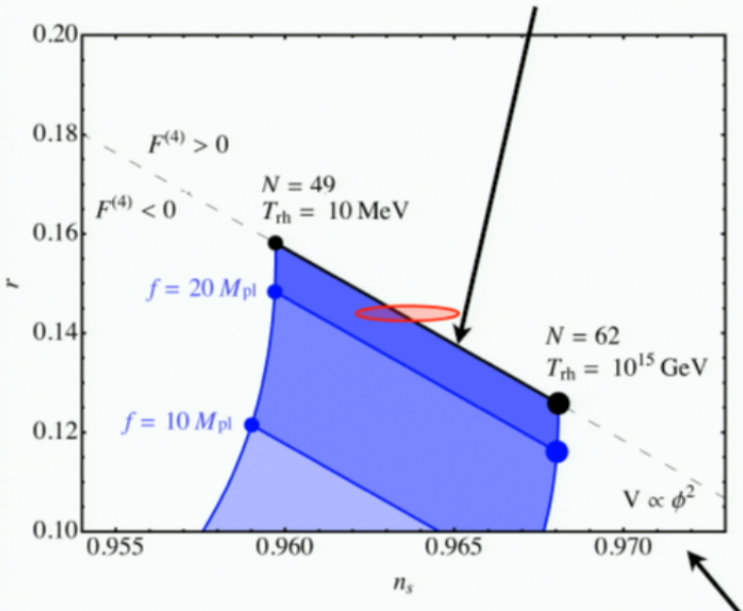

FIG. 1: *Future constraints on f assuming a simple cosine potential. The dashed curve corresponds to Eq. (1) and the black segment covers the interval of reheating temperatures $T_{rh} \in [10\,\mathrm{MeV}, 10^{15}\,\mathrm{GeV}]$. A wider range of N is allowed if one considers non-standard cosmological evolutions after inflation. Red 1σ contour corresponds to a futuristic measurement with $\sigma_{n_s-1} = \sigma_r = 10^{-3}$, compatible with a quadratic potential.*

- Crucial to measure ns better
- Error in N around 0.4
- Constraints on small departures:

$$V(\phi) = \Lambda^4 \left(1 - \cos\left(\frac{\phi}{f}\right)\right) \rightarrow f > 30 M_{pl}$$

$$(\partial\phi)^4 / \Lambda^4 \rightarrow \Lambda \gtrsim 2 \cdot 10^{16}\ \mathrm{GeV}$$

$$c_s^2 - 1 = 16 \frac{\dot{H} M_{pl}^2}{\Lambda^4}$$

- Running for consistency

$$V \propto \phi$$

Lives outside the plot !